EXAMINATION OF DELAMINATION MIGRATION THROUGH MICRO-SCALE SIMULATION

David Mollenhauer[1], Eric Zhou[2] , Endel Iarve[3], Michael Braginsky [2], Kevin Hoos[3], Tim Brietzman[1] and Dan Rapking[4]

[1]Air Force Research Laboratory, Wright Patterson AFB, Ohio, USA
Email: david.mollenhauer@us.af.mil
[2]University of Dayton Research Institute, Dayton, Ohio, USA
[3]University of Texas at Arlington, Arlington, Texas, USA
[4]Wright State University, Fairborn, Ohio, USA

Keywords: delamination, migration, X-FEM, fracture, micro-scale

Abstract
A Discrete Damage Modeling (DDM) approach using a Regularized eXtended-Finite Element Method (Rx-FEM) formulation has been applied to a test specimen for characterizing delamination migration in laminated composites. The migration specimen is designed such that as a delamination propagates, the stress state alters such that delamination migration through a neighboring ply becomes favorable. The present research aims to use the DDM framework to simulate the local, micro-scale behavior at a delamination migration point. Additional functionality to the Rx-FEM formulation, required for this task, allows for Rx-FEM cracks of arbitrary shape. A four-point shear fracture specimen was used as empirical guidance in validating this capability. Excellent agreement between model and experiment was shown. A laminated effective-modulus representation of the test was then modeled using the DDM framework, establishing the point of delamination migration. Location of delamination migration was predicted accurately. A local, micro-scale model was constructed and applied at the location of migration. The micro-scale model consisted of arbitrary interacting cracks in resin-rich zones using the modified Rx-FEM formulation and standard cohesive zone disbonding between fibers and resin. Model predictions show great similarity to the initial shape of the migrating transverse cracks observed in experiment.

1. Introduction

Recent developments in the simulation of damage evolution in laminated composites have allowed the representations of matrix damage in a discrete manner [1]. That is, matrix cracks are modeled explicitly in a mesh-independent manner and are allowed to interact with each other and delaminations between plies. This DDM approach has been applied to a variety of laminated and textile composite configurations, including to a test specimen for characterizing delamination migration in laminated composites [2,3]. The migration specimen, shown in Figure 1, consists of a cross-ply stacking sequence with a teflon starter delamination below a central set of 90-degree plies. As the delamination propagates, the stress state becomes favorable for the delamination to migrate to the top of the central 90-degree plies. This migration location is a function of specimen geometry and loading type (static or fatigue) [4]. The aim of the present research was to use the DDM framework to simulate the local, micro-scale behavior at a delamination migration point in the migration test specimen. Additional functionality to the Rx-FEM formulation, required for this task, allows for Rx-FEM cracks of arbitrary shape and is described subsequently. Validation of Rx-FEM simulations of cracking using a four-point shear experiment is shown. Finally, a global-local modeling effort to demonstrate the DDM framework at an effective modulus scale and at a micro-scale will be described.

Excerpt from ISBN 978-3-00-053387-7

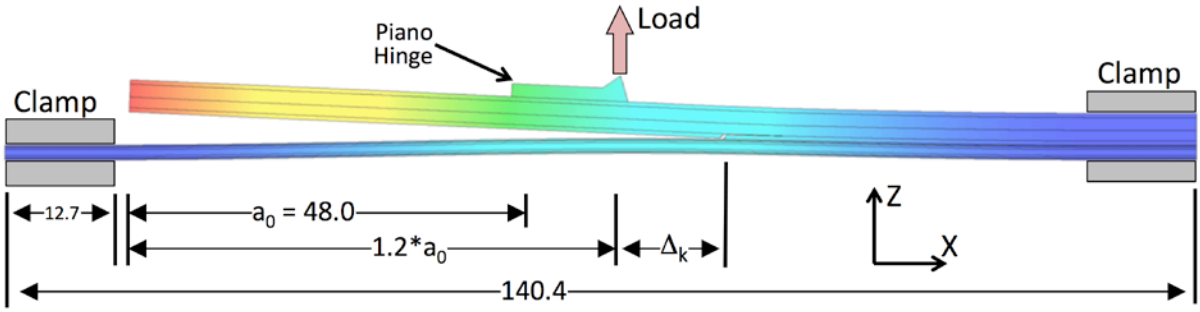

Figure 1. Deformed image of a migration specimen simulation (all dimensions in mm).

2. Rx-FEM with Arbitrary Curvature

The Regularized eXtended Finite Element Method (Rx-FEM) allows for the modeling of displacement discontinuities associated with individual cracks in a general 3D setting, without regard to mesh orientation, by inserting additional degrees of freedom in the process of the simulation [1]. This methodology is a variant of the X-FEM where the Heaviside step function is replaced by a continuous approximation. The propagation of the mesh independent crack is then performed by using a cohesive zone method of the type described in [5]. This technique was extensively used in laminated composites where crack orientation is predefined by fiber orientation. Recently it was used in conjunction with three dimensional failure criterion LARC04, which allowed to define the crack orientation in the plane transverse to the fiber orientation [6]. In the present paper we are extending the approach to arbitrary 3D cracking. Two aspects of the cracking problem were addressed to facilitate this capability, the crack orientation and the extension modeling. The crack orientation was defined perpendicular to the direction of the maximum principal stress. This orientation was calculated in every integration point at the end of each converged load step and used to insert a cohesive zone for crack propagation along this predefined curved path (see Figure 2). The crack extension, and more precisely, the cohesive zone insertion length was determined by the value of the failure criterion. A threshold value of the failure criterion close to 1 was selected and the cohesive zone extended along the predefined curved path in the area where the threshold value of the failure criterion was exceeded. The crack opening was then allowed to proceed along this path as defined by the parameters of the cohesive zone. This process was repeated on each load step.

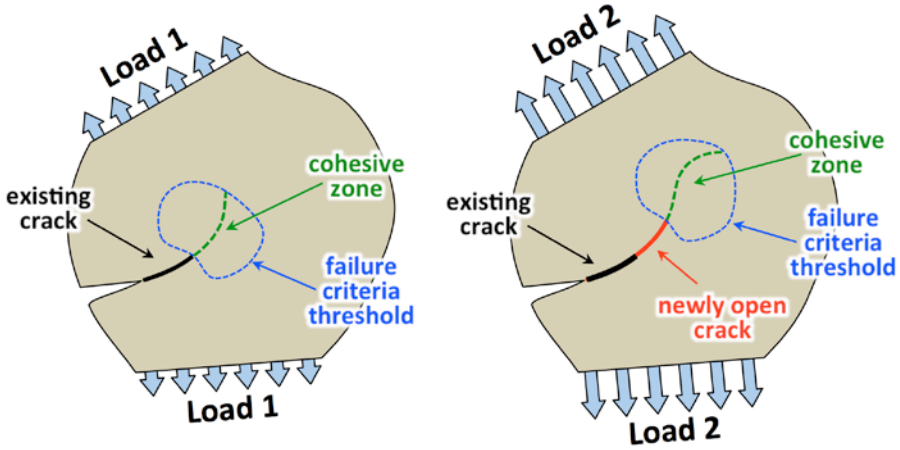

(a) (b)

Figure 2. Schematic of the arbitrary Rx-FEM cracks on two sequential load steps. In (a), the maximum principal stress field is used to extend a cohesive zone to a pre-defined failure criteria threshold value and the crack is allowed to open. In (b), the process is repeated for the next load step.

Excerpt from ISBN 978-3-00-053387-7

3. Four-Point Shear – Validation of Arbitrary Crack Methodology

The Single-Edge-Notch (SEN) specimen, loaded in 4-point shear, was proposed as a round-robin test specimen by Carpinteri, et. al. [7] for examining mixed mode crack growth in concrete. Two SEN specimen sizes were described in detail in Schlangen [8]. In the present work, the smaller beam configuration was examined. The specimen was modeled (see Figure 3) using the above described damage framework and loaded incrementally in displacement control. Growth of the Rx-FEM cracks is governed by a cohesive zone formulation described in Turon [5]. The modeled beam matched the specified dimensions (400mm long, 100mm tall, and 100mm thick) with the exception of the thickness, which was modeled as 1 mm thick. Table 1 shows the material properties applied to the model to represent a normal-weight concrete. Schlangen reported significant load-displacement behavior sensitivity and, to a lesser extent, crack path sensitivity to the applied boundary conditions. The two boundary condition configurations described in [8], fixed or freely-rotating loading noses, were modeled, however for brevity, only the freely-rotating results are presented herein. The model mesh (not shown) was refined to and average element size of 1.0mm in a rectangular region at the center of the specimen and was produced with the open-source meshing program Gmsh [9].

Table 1. Normal-weight concrete properties applied to model.

E_1 (GPa)	ν	X_t (MPa)	X_c (MPa)	S (MPa)	G_{Ic} (N/mm)	G_{IIc} (N/mm)
35.0	0.15	3.0	30.0	18.0	0.10	1.00

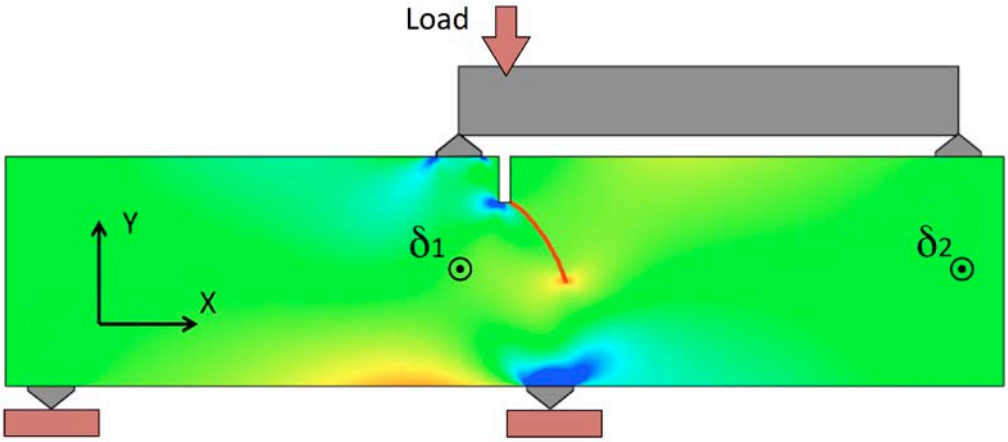

Figure 3. SEN specimen as modeled showing four freely-rotating loading noses, load introduction beam, displacement measurement locations (δ_1, δ_2), crack path at peak loading (red line), and X-direction stress field (±10 MPa).

The X-direction stress field is shown in Figure 3 at the point of maximum load. The curved crack path, shown in red, terminates with an obvious stress concentration. Modeled and experimental [8] load-displacement results at points δ_1 and δ_2 are shown in Figure 4. Considering the sensitivity of the behavior to the nature of the boundary conditions, these results were deemed acceptable. Figure 4 also shows a close-up of the central region of the modeled SEN beam at the final load step. The experimentally observed cracking patterns in Schlangen [8] showed variable behavior, likely due to the average 8mm stone aggregate in the concrete beams tested. The experimentally observed crack variation is represented by the grey band superimposed on the specimen image. The predicted path fits within the band of observed cracking.

Excerpt from ISBN 978-3-00-053387-7

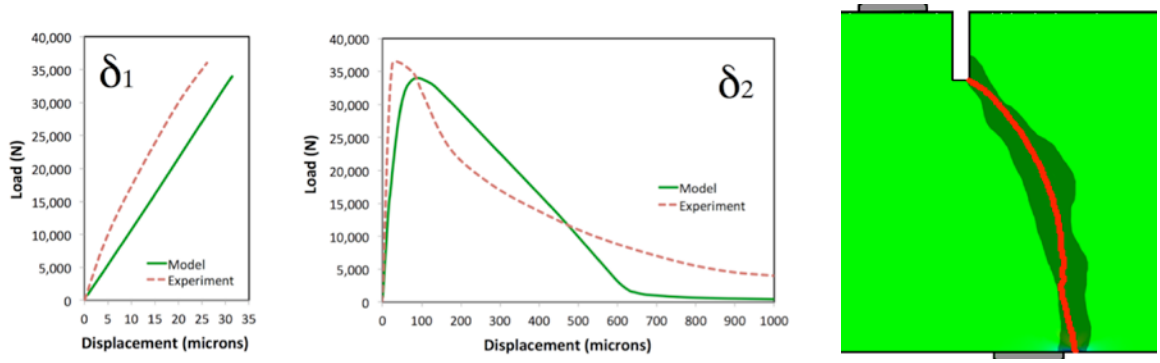

Figure 4. Modeled and experimental load-displacement curves at locations δ_1, and δ_2, and final predicted crack path (red) with experimental extents of cracking from multiple tests (grey).

4. Single Cantilever Beam – The Delamination Migration Specimen

4.1. Effective-Modulus Model and Results

A migration specimen of the type described in [2,3] was modeled using the DDM framework using effective-modulus representations of each ply. The test specimens were manufactured with an IM7/8552 unidirectional material with a stacking sequence of [$0_4/90_{12}/0_{10}/90_4$/ T/$0/90/0_2/90_6/0_2/90/0$], where "T" represents a Teflon insert that acts as an initial delamination starter in the region labeled a_0 in Figure 1. Reference [3] describes conducting tests with several different locations of the loading location with respect to the initial delamination tip location. In this study, only the $1.2*a_0$ case was examined. Table 2 details the material properties used in the model. Boundary conditions were applied such that the clamped regions were restricted in both X and Z. Load was applied to a single row of nodes at the apex of the "piano-hinge" shown in Figure 1 (at X=72.5mm), allowing free rotation of the upper part of the cantilever beam. The test specimens were 12.7mm in width while the modeled width was 1.0 mm with the front and back faces fixed in Y. Meshing was again accomplished using Gmsh with a refined region spanning in X from 82.0 mm to 91.0 mm in the 90° ply targeted for migration. Average element size within this region was 0.04 mm. In addition to delamination capabilities between plies, the capability of an arbitrarily curved Rx-FEM crack was enabled, both governed by the properties listed in Table 2.

Table 2. IM7/8552 model properties.

E_1 (GPa)	E_2 ,E_3 (GPa)	G_{23} (GPa)	G_{12} ,G_{13} (GPa)	ν_{23}	ν_{12}, ν_{13}	*ply* (mm)
161.0	11.4	3.98	5.17	0.44	0.32	0.125

X_t (MPa)	X_c (MPa)	X_t (MPa)	Y_c (MPa)	S (MPa)	G_{Ic} (N/m)	G_{IIc} (N/m)
2323	2068	60.0	276.0	90.0	200	1000

Figure 5 shows a close-up of the migration region and details of the mesh surrounding the refined migration region. The predicted migration point (Δ_k in Figure 1) was ~12.2 mm from the load application point while the experimental average was reported to be 12.5 mm. Average angle of the migrating crack was ~51° and the experimentally measured average value for this configuration was ~52°. Recall that the X location and the shape of this transverse crack that allows the delamination to migrate was not specified, but predicted using the DDM framework

Excerpt from ISBN 978-3-00-053387-7

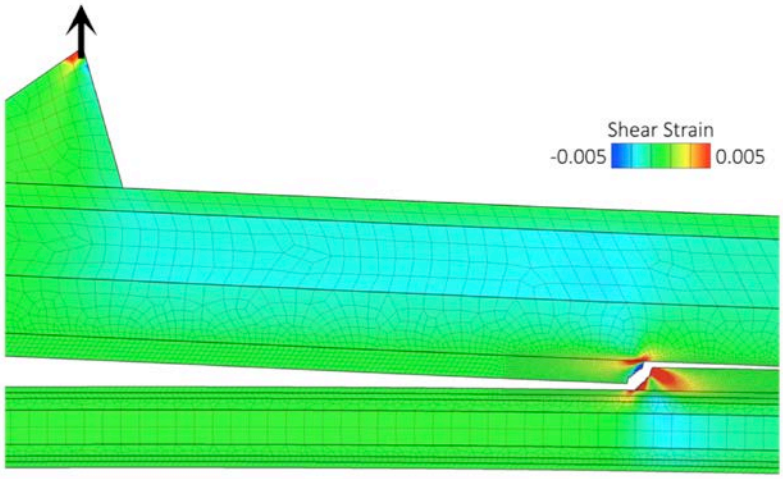

Figure 5. The central region of the modeled SCB specimen showing the migration location and mesh.

A close-up of the migration location just prior to the formation of the transverse crack in the 90_4 ply stack is shown in Figure 6. For reference, this figure shows the future path of the crack. Also shown in the figure is the region encompassed by the local, micro-scale model to be discussed in the next section. To enable the global-local modeling desired, displacements were extracted from the boundary of this rectangular region for application to the boundaries of the local model. Rigid body translations and rotations were minimized, resulting, coincidentally, in the right edge of the rectangular region showing essentially no variation in X-direction displacements.

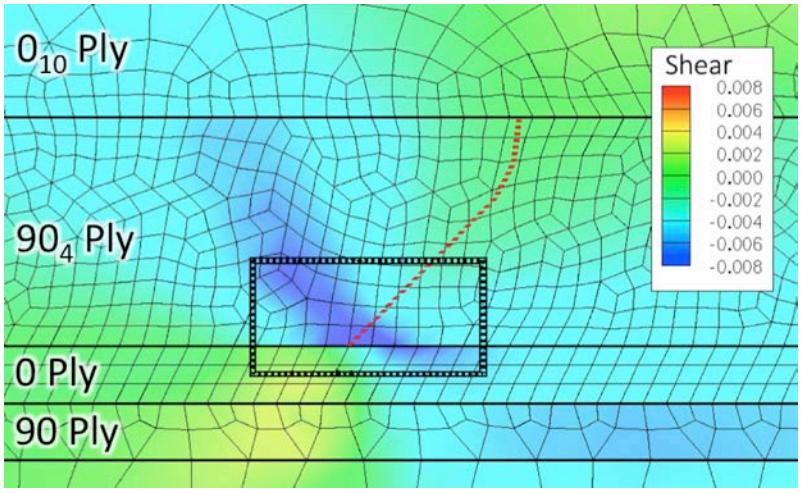

Figure 6. Close-up of migration region just prior to initiation of the migration transverse crack (future crack path is shown in red). The local analysis region is bounded by the black, rectangular hatching.

4.2. Micro-scale Model and Results

A local model was developed encompassing the rectangular section shown in Figure 6. It consisted of a sections of both the 0° ply below and the 90° ply above the delaminating interface (see Figure 7). The 0° ply thickness was 62.5 μm while the 90° ply thickness modeled was 187.5 μm. The left edge of the rectangle was 230 μm from the point of migration while the length of the rectangular region was 500 μm. A 50 μm by 50 μm square micro-scale geometry was embedded within the local model such that the left edge of the micro-geometry was 12 μm from the end of the delamination. This micro-scale geometry consisted of 70 fibers with 5 μm diameters representing the IM7 fibers of the tested

Excerpt from ISBN 978-3-00-053387-7

specimens and had an average fiber volume fraction of 55%. Material properties of the constituents are listed in Table 3, while the surrounding plies regions use those properties listed in Table 2. Stiff, thin "boundary condition" blocks were added to the top, the bottom, and the left side of the local model for ease of applying the displacement distributions obtained from the global model. Eleven points along each of the top and bottom and eight points along the left were chosen and assigned appropriate displacements. The model was then allowed to increase the displacements gradually from zero in 5% increments until the full magnitude of the global displacements was applied.

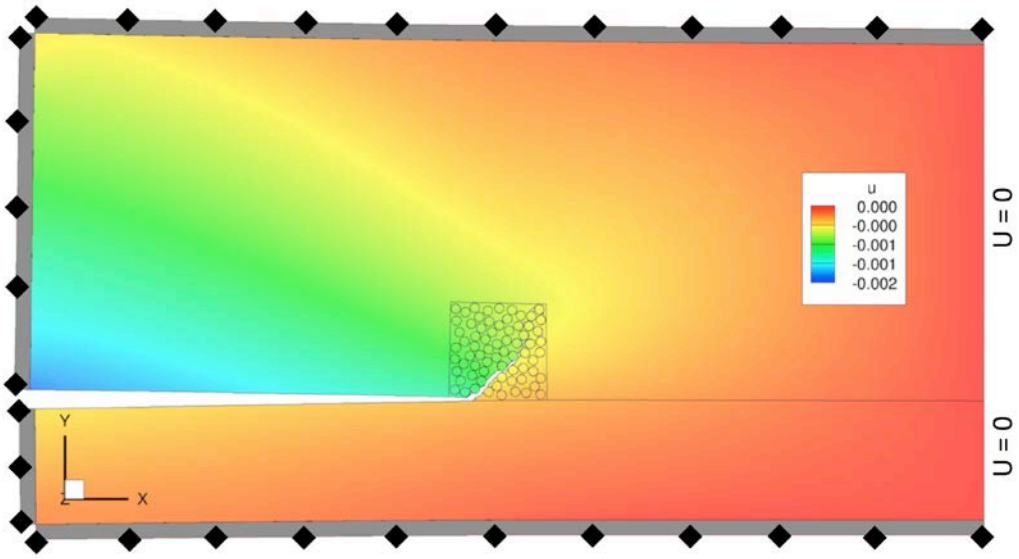

Figure 7. Local model showing Rx-FEM damage growing through the embedded micro-scale geometry. The grey bars (top, bottom, and left) are stiff "boundary condition" blocks with point displacements applied at the black diamond locations.

Table 3. Constituent properties used in the micro-scale region of the local model.

	E_1 (GPa)	E_2 (GPa)	ν_{23}	ν_{12}, ν_{13}	G_{23} (GPa)	G_{12} ,G_{13} (GPa)	X (MPa)	S (MPa)	G_{IIc} (N/m)
Resin	3.45	-	0.35	-	1.28	-	77.0	42.0	177
Fiber	276.0	27.6	0.8	0.3	7.67	138	-	-	-
Interface	-	-	-	-	-	-	69.0	38.0	140

The micro-scale geometry region of the local model consists of fibers and resin and the interface between them. The DDM allows for disbonding between fibers and resin while also allowing arbitrarily curved Rx-FEM cracks within the resin regions. Growth of damage in both are governed by the cohesive formulation of [5] with slightly reduced interfacial properties as shown in Table 3. Displacement and damage results are shown in Figure 8. Open, Rx-FEM cracks are indicated by white space where elements have been omitted if their cohesive zone damage variable exceeds 0.975. An initial coalesced crack seems to dominate from the delamination tip at an angle of approximately 45°, smaller than the average migration crack observed in experiment. However, generally the initial, migrating crack emanates from the delamination tip at a shallower angle than the average of the whole migration crack. This is evident in magnified images presented in [3]. The single, dominant crack seems to fragment as the upper right corner of the micro-geometry region is approached. This is likely due to a mismatch in the micro-geometry properties and the properties of the homogenized regions, which were not allowed to fail in this simulation.

Excerpt from ISBN 978-3-00-053387-7

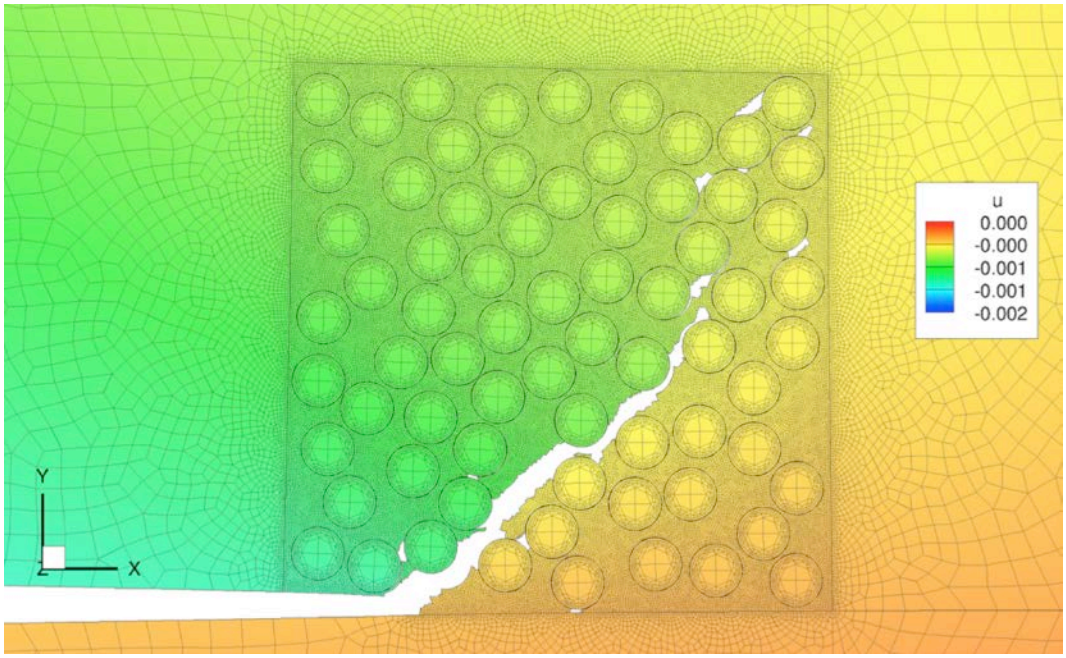

Figure 8. Deformed image of the damage evolution through the micro-scale geometry. Elements where the cohesive zone damage variable exceeds 0.975 are removed. Displacements are in mm.

5. Conclusions

A global-local modeling effort was presented with the aim of representing delamination migration at the micro-scale. A new, arbitrarily curved Rx-FEM approach was presented and demonstrated against a reference fracture specimen loaded in 4-point shear, exhibiting an excellent match to experimental results. The global, effective-modulus model of the migration specimen was shown to be effective in producing the delamination migration at the correct geometric location on the specimen and at the correct angle. A local, mixed effective-modulus and micro-scale constituent-level model was also shown to exhibit the proper fracture tendencies, when compared to experimental results. Future efforts will incorporate larger micro-scale volumes to understand the constituent-level fracture process over a longer length scale.

Acknowledgments

This work is a result of continuous and periodic funding from a number of organizations. These included the U.S. Air Force Research Laboratory Materials and Manufacturing Directorate, the U.S. Air Force Office of Scientific Research (Multiscale Structural Mechanics program, Dr. David Stargel), and NASA Langley Research Center (Dr. Kevin O'Brien and Dr. James Ratcliffe).

References

[1] E. Iarve and D. Mollenhauer. *Numerical Modeling of Failure in Advanced Composite Materials, 1st Edition, Chapter 9: Mesh-Independent Matrix Cracking and Delamination Modeling in Advanced Composite Materials*. eds. P. Camanho and S. Hallett. Woodhead Publishing, 2015.

[2] J. Ratcliffe, M. Czabaj, and K. O'Brien. A Test for Characterizing Delamination Migration in Carbon/Epoxy Tape Laminates. *NASA/TM-2013-218028,* 2013.

Excerpt from ISBN 978-3-00-053387-7

[3] J. Ratcliffe and N. De Carvalho. Investigating Delamination Migration in Composite Tape Laminates. *NASA/TM-2014-218289*, 2014.

[4] E. Iarve, K. Hoos, and D. Mollenhauer. Discrete Damage Simulation and Measurement in Composite Laminates under Fatigue Loading. *Proceedings of the 16th European Conference on Composite Materials, Seville, Spain,* 22-26 June 2014.

[5] A. Turon, P. Camanho, J. Costa, and C. Davila. A Damage Model for the Simulation of Delamination in Advanced Composites under Variable-Mode Loading. *Mechanics of Materials*, 38:1072-89, 2006.

[6] S. Pinho, C. Dávila, P. Camanho, L. Iannucci, and P. Robinson. Failure Models and Criteria for FRP under In-Plane or Three-Dimensional Stress States Including Shear Non-Linearity. *NASA/TM-2005-213530*, 2005.

[7] A. Carpinteri, G. Ferrara, and G. Melchiorri. *Fracture of Concrete and Rock – Recent Developments: Single Edge Notched Specimen Subjected to Four Point Shear: an Experimental Investigation*. eds. S. Shah, S. Swartz, and B. Barr. Elsevier Applied Science Publishers, 1989.

[8] E. Schlangen. *Experimental and Numerical Analysis of Fracture Processes in Concrete.* TU Delft. Delft University of Technology, 1993.

[9] C. Geuzaine and J. Remacle. Gmsh: a Three-dimensional Finite Element Mesh Generator with Built-in Pre- and Post-processing Facilities. *International Journal for Numerical Methods in Engineering*, 79:1309-1331, 2009.

Excerpt from ISBN 978-3-00-053387-7